Proc. Natl. Acad. Sci. USA
Vol. 75, No. 6, pp. 2829–2833, June 1978
Cell Biology

Comparison of *Artemia salina* and *Escherichia coli* ribosome structure by electron microscopy

(eukaryotic–prokaryotic ribosome/structural similarity)

M. BOUBLIK AND W. HELLMANN

Roche Institute of Molecular Biology, Nutley, New Jersey 07110

Communicated by Severo Ochoa, April 6, 1978

ABSTRACT **The structure of eukaryotic *Artemia salina* and prokaryotic *Escherichia coli* ribosomes has been compared by electron microscopy. Despite the established differences in size and in the amount and proportion of the protein and RNA moieties, both types of ribosomes appear to have substantial similarity in the overall shape and in the mutual orientation of the subunits on the monosome. The small subunit is located in the "crown" region of the large subunit lengthwise between the two side crests. However, high-resolution electron microscopy reveals distinct differences in the fine structure of both small and large subunits. The 40S *A. salina* subunit with three structural domains is more complex than the corresponding *E. coli* subunit. The 60S *A. salina* subunit has a less expressed "crown" region and shows a knob-like protrusion in the base. Structural asymmetry is a characteristic feature common to subunits and monosomes from both *A. salina* and *E. coli***

The structural complexity of ribosomes results from their large number of constituents. The simplest known ribosome, the 70S *Escherichia coli* monosome, consists of 53 different proteins and 3 ribonucleic acid molecules. Twenty-one proteins and one RNA (16S) molecule are present in the small (30S) subunit; thirty-two proteins and two RNAs (23S and 5S) make up the large (50S) subunit (see refs. 1 and 2 for recent reviews). Although the composition of eukaryotic ribosomes is similar, the larger ribonucleic acids (28S, 18S, and 5.8S) and the more than 70 ribosomal proteins (3) imply a greater complexity.

A general similarity in the structure of eukaryotic and prokaryotic ribosomes has already been suggested in earlier electron microscopic studies (4). Progress in isolation of ribosomes and characterization of their constituents and improvement in electron microscopic techniques enable us to investigate the three-dimensional structure of ribosomes at a higher level of resolution. In this study we have compared the structural resemblance of ribosomal particles from *E. coli*, a classical prokaryote, and from *Artemia salina*, a convenient source of eukaryotic ribosomes (see ref. 5 for refs.).

MATERIALS AND METHODS

Ribosomes and Ribosomal Subunits. 80S monosomes and 60S and 40S subunits were prepared from *A. salina* embryos (Metaframe, San Francisco Bay Brand II 503-3) by the procedure of Zasloff and Ochoa (5). Ribosomes and subunits were stored at −20° in 20 mM 4-(2-hydroxyethyl)-1-piperazineethanesulfonic acid (Hepes) (pH 7.5)/100 mM KCl/5 mM magnesium acetate/0.1 mM EDTA/1.0 mM dithiothreitol (buffer A) in 50% glycerol (vol/vol). 70S monosomes and 50S and 30S subunits were prepared from *E. coli* as described (6, 7). They were stored in 10 mM Tris·HCl (pH 7.4)/10 mM $MgCl_2$/10 mM NH_4Cl (buffer B) at 4°C or in liquid nitrogen.

Electron Microscopy. Specimens for electron microscopy were prepared as described (8). A 0.5% aqueous uranyl acetate solution was used as a contrasting solution. The grids were examined in a JEM 100B electron microscope operated at 80 kV and a direct magnification of ×70,000. The tilting experiments were performed with a JEM 100C equipped with a side entry goniometer stage. Printing was done with the plate emulsion facing the paper emulsion. The dimensions of the subunits and the monosomes were determined by measuring highly enlarged electron micrographs of about 300 ribosomal particles deposited by the modified sandwich technique (8).

RESULTS

Overall views of ribosomal particles (Figs. 1*A*–6*A*) reflect merely the quality of the preparation and the degree of preferential orientation on the carbon support. Contours and electron density patterns, the main criteria for the fine structure of ribosomes, are more clearly visualized on enlarged electron micrographs of selected particles. They were obtained mostly by the adsorption technique (8), which explains the inconsistencies in size. Schematic drawings represent simplified structural features typical of the ribosomal particles under study.

Small subunits

An overall field of *A. salina* 40S subunits (Fig. 1*A*) is supplemented by a gallery of selected electron images of subunits at a higher magnification (Fig. 1*B*). The elongated contours reflect orientation on the supporting carbon film on the grid. The particles predominantly assume one of two positions, referred to as "frontal" and "lateral." Both views indicate asymmetry in the shape of the subunit.

Subunits in the frontal position (Fig. 1*B 1* and *6*) resemble the small subunits of *E. coli* in the corresponding views (Fig. 2*B*). The only obvious difference is in size; *A. salina* 40S subunits are larger (250 × 125 Å ± 10%) than *E. coli* 30S subunits (220 × 100 Å ± 10%). However, the ratio between the largest and the smallest dimension remains close to ~2 for both small subunits.

Lateral views of the subunits, which are slightly prevalent, reveal remarkably complex topographic patterns (Fig. 1*B 2–5* and *7–9*) although no obvious preference for either side is observed. Electron-dense grooves imply the existence of at least three distinct structural segments, with a beak-like protrusion in the "upper" third of the 40S subunit. The schematic drawing (Fig. 1*B 10*) demonstrates the structural details of the lateral views.

An overall view of 30S *E. coli* subunits is shown in Fig. 2*A*. Their typical morphological features—the elongated profile,

The costs of publication of this article were defrayed in part by the payment of page charges. This article must therefore be hereby marked "*advertisement*" in accordance with 18 U.S.C. §1734 solely to indicate this fact.

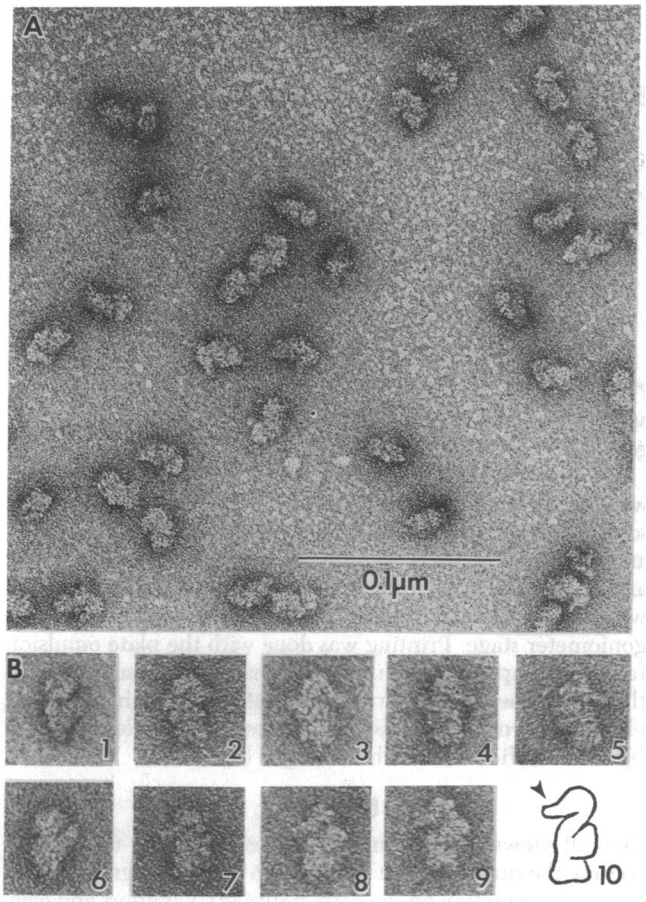

FIG. 1. 40S ribosomal subunits from *A. salina* in buffer A, stained with 0.5% aqueous uranyl acetate. (*A*) Overall view. (×271,600.) (*B*) Selected particles in frontal (*1* and *6*) and lateral (*2–5* and *7–9*) views. (×407,400.) Schematic drawing (*10*); arrow points to the beak-like protrusion.

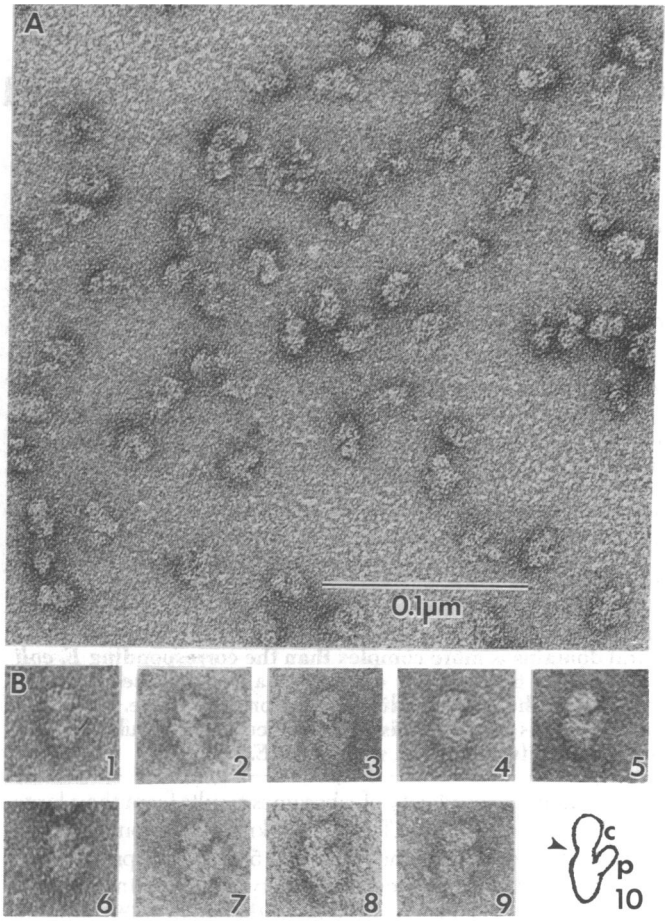

FIG. 2. 30S ribosomal subunits from *E. coli* in buffer B, stained with 0.5% aqueous uranyl acetate. (*A*) Overall view. (×280,000.) (*B*) Selected particles (*1–9*). (×420,000.) Schematic drawing (*10*): c denotes the cleft; arrow, the "one-third" partition; p, the platform.

the "one-third" partition (9), the cleft, and the platform (10) —are better seen in the highly enlarged electron images in Fig. 2*B 1–9*. The subunits have a slight preference for an orientation with the cleft on the right-hand side, schematically shown in Fig. 2*B 10*. The platform is the most evident feature of asymmetry. Structures similar to the lateral views of 40S *A. salina* subunits (Fig. 1*B*) were not observed on 30S *E. coli* subunits (Fig. 2A).

Large subunits

60S *A. salina* subunits are seen in an overall view of the electron micrograph in Fig. 3*A* as round particles with a diameter of about 260 Å ± 10%. The diversity of projections suggests no obvious preferential orientation of the subunits on the carbon support. On the other hand, 50S *E. coli* subunits (Fig. 4), with a diameter of 225 Å ± 10%, exhibit a strong preferential orientation for the "crown" view (9).

The limited variety of views of 50S *E. coli* subunits makes a complete structural comparison of *A. salina* and *E. coli* subunits rather difficult. Therefore, our study has been focused on the morphology of both large subunits in the crown view. A gallery of electron images of selected large *A. salina* subunits in this view is in Fig. 3*B 1–5*, that of *E. coli* in Fig. 4*B 1–9*. The crown, as described for 50S *E. coli* subunits (9, 11, 12), consists of three crests (Fig. 4*B 10*). The middle crest and the left-hand side crest are present on both large *A. salina* and *E. coli* subunits to a comparable extent. The left-hand side crest, 100–150 Å long, shows variable orientation and is the dominant feature of the asymmetry of the large subunits. A split at the end of the crest can be occasionally resolved in both 50S and 60S subunits. The right-hand side crest of the 60S subunit appears less expressed than in the 50S subunit, enhancing the roundness of the *A. salina* particle. However, the most significant structural difference between the subunits in the crown view is a knob-like protrusion of about 50 × 40 Å in the base of the 60S *A. salina*. The schematic drawing (Fig. 3*B 10*) shows the described structural features of large *A. salina* subunits more explicitly. Fig. 3*B 6–9* shows electron images of 60S *A. salina* particles in various views.

Monosomes

80S *A. salina* and 70S *E. coli* monosomes appear in the electron micrographs (Figs. 5*A* and 6*A*) as round-shaped particles with a diameter of 260 Å ± 10% and 225 Å ± 10%, respectively. The electron-dense groove, visible on the majority of the monosomes in various projections depending on their orientation on the support, indicates the interface between the large and small subunit. Unfortunately, the heavy stain deposit, which makes the interface on the electron micrographs so prominent, obscures all structural details.

The study of the interface is thus limited to the determination of the mutual position of the subunits. The view in which the orientation of both subunits on the monosome is most clearly seen corresponds to the crown view of the large subunits (Figs. 3*B 1–5* and 4*B 1–9*). Selected images of *A. salina* monosomes (Fig. 5*B 1–9*) show the small subunit to be oriented lengthwise

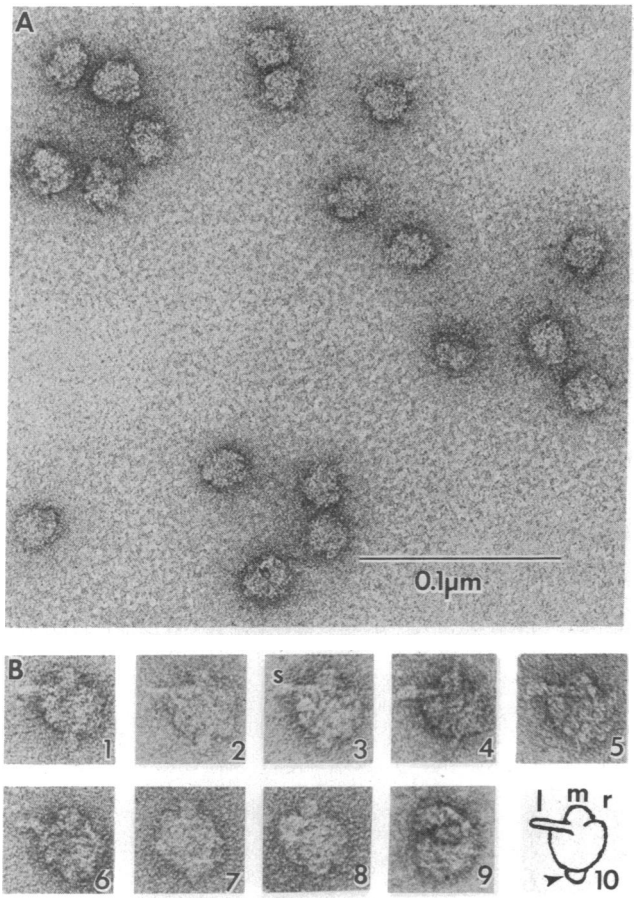

FIG. 3. 60S ribosomal subunits from *A. salina* in buffer A, stained with 0.5% aqueous uranyl acetate. (*A*) Overall view. (×271,600.) (*B*) Selected particles in the crown view (*1–5*) and in various views (*6–9*). (×407,400.) Schematic drawing (*10*): m denotes the middle crest; r, the right-hand side crest; l, the left-hand side crest (with the split, s); arrow indicates the protrusion in the base.

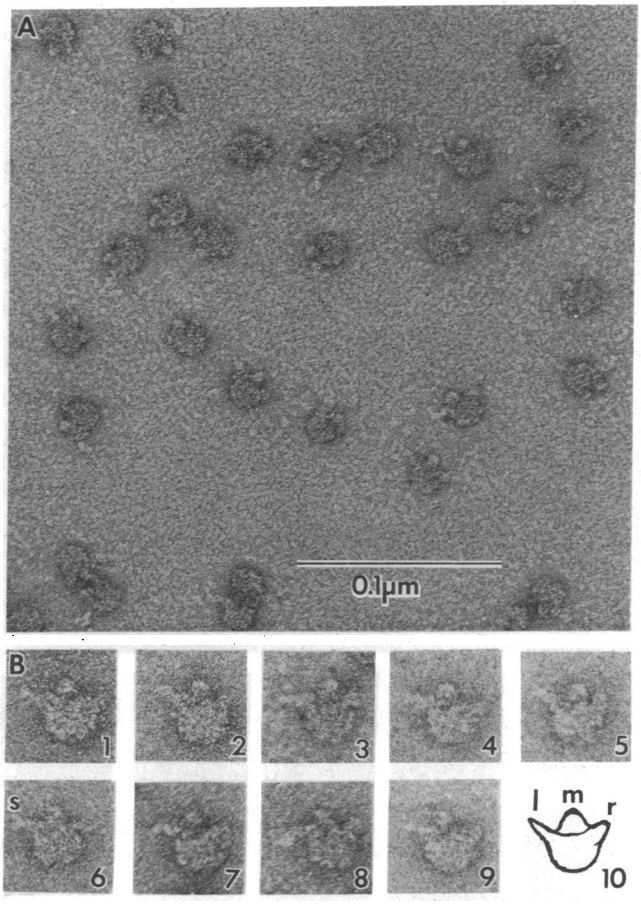

FIG. 4. 50S ribosomal subunits from *E. coli* in buffer B, stained with 0.5% aqueous uranyl acetate. (*A*) Overall view. (×271,600.) (*B*) Selected particles in the crown view (*1–9*). (×407,400.) Schematic drawing (*10*): l, s, m, and r refer to the left-hand side crest, the split, the middle crest, and the right-hand side crest, respectively. Notice the variety in shapes and orientation of the left-hand side crest.

in the crown region of the large subunit between the two side crests, with the one-third partition directed toward the left-hand side crest. A similar arrangement of the subunits is also observed in the *E. coli* 70S monosome (Fig. 6*B 1–9*). Structural features of *A. salina* and *E. coli* monosomes are shown schematically in the Figs. 5*B 10* and 6*B 10*, respectively. Apart from size, the main difference evident from comparison of *A. salina* and *E. coli* monosomes in the crown views is a protuberance seen on some of the 60S *A. salina* subunits (Fig. 5*A 2* and *7*). The knob-like protrusion in the base of the 60S *A. salina* subunit (Fig. 3*B*) has not yet been observed on the 80S monosome in the corresponding view (Fig. 5*B*). Surprisingly, a similar protrusion can be sometimes resolved in the base of *E. coli* monosomes (Fig. 6*B 4*).

The small differences in size between the large subunits and the monosomes make it difficult to distinguish these particles in certain positions. This drawback should be eliminated by specimen tilt. A proper tilt should also overcome the limit of views caused by preferential orientation of ribosomal particles. However, tilting is a demanding electron microscopic technique seldom applied to the structural study of ribosomes (9, 13). The experimental difficulties usually reside in finding the axis of the tilt and the correct focus. Beam damage of the specimen by multiple exposure is an additional factor for consideration. In our experience the most meaningful structural information can be obtained with a tilt of ±45° along two mutual perpendicular axes. The quality of electron micrographs (Fig. 7) obtained under these conditions suffers from the mentioned drawbacks; however, the additional information is still very valuable. *A. salina* monosomes in the crown view were tilted ±45° along the vertical (Fig. 7*A*) and the horizontal (Fig. 7*B*) axes. The tilting reveals that the apparent roundness of *A. salina* monosomes (Fig. 5*A*) is a consequence of preferential orientation; 80S monosomes are actually slightly prolate, as are *E. coli* 70S ribosomes (8). 80S particles in the +45° tilt (Fig. 7*A*) closely resemble 60S subunits.

DISCUSSION

The aim of this electron microscopic study was to compare the size and structure of ribosomes from two different classes—eukaryotic of *A. salina* and prokaryotic of *E. coli*.

The size of ribosomes is important both as a morphological parameter and as a framework for topographical mapping. However, the dimensions of ribosomes as obtained by electron microscopy are somewhat inconsistent (see ref. 2 for review); variation of the mode of specimen deposition, staining, and dehydration conditions are the primary causes of these discrepancies. In our hands the most reproducible data on the size of ribosomes can be obtained by the sandwich technique (8). Ribosomal particles mounted by this procedure are protected against beam damage by the additional carbon film and by the even "embedding" in the contrasting solution (uranyl acetate). Therefore, they appear larger than particles deposited by the conventional technique on a single support. By mounting ri-

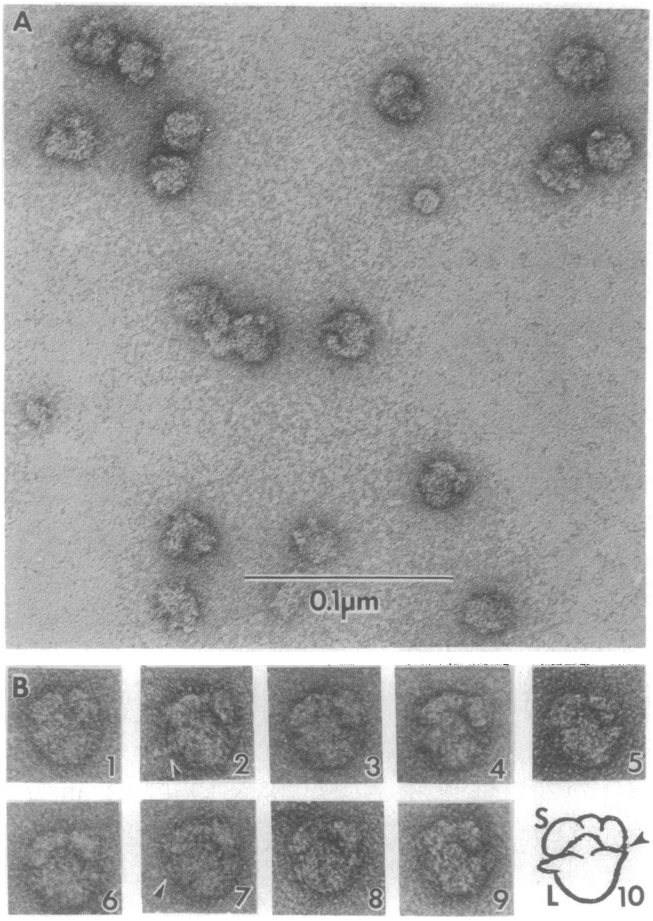

FIG. 5. 80S ribosomes from *A. salina* in buffer A, stained with 0.5% aqueous uranyl acetate. (*A*) Overall view. (×280,000.) (*B*) Selected particles in the crown view (*1–9*); arrows in *2* and *7* point to the protuberance on the large subunit. (×420,000.) Schematic drawing (*10*): S refers to the small subunits; L, the large subunits; arrow points to the interface.

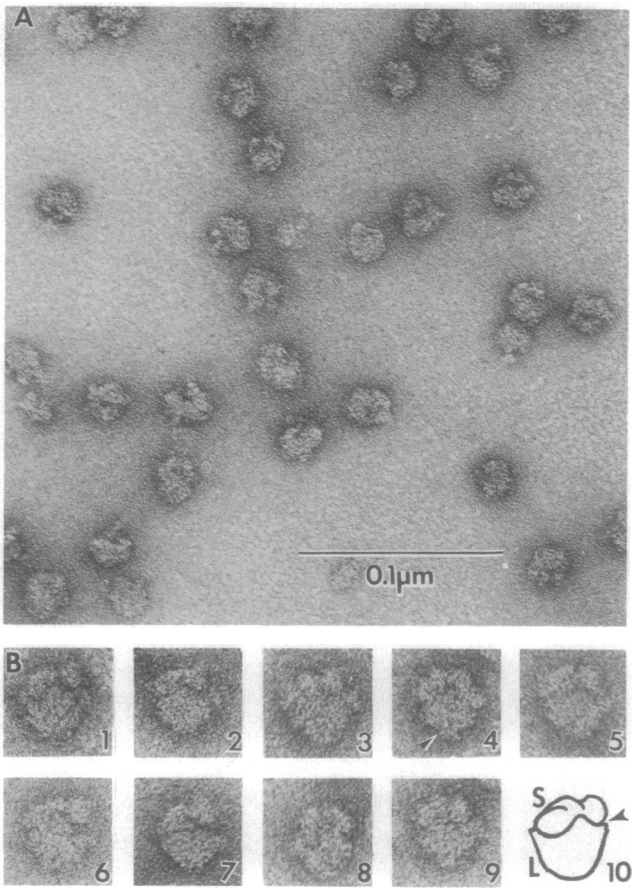

FIG. 6. 70S monosomes from *E. coli* in buffer B, stained with 0.5% aqueous uranyl acetate. (*A*) Overall view. (×271,600.) (*B*) Selected particles in the crown view (*1–9*); arrow in *4* points to the protrusion in the base. (×407,400.) Schematic drawing (10). Symbols have the same meaning as in Fig. 5*B*.

bosomes in various modes and using tobacco mosaic virus as a size and stability marker, we have already shown (8) that the additional carbon film has no flattening effect on the ribosomes (10). Statistical evaluation of electron images of ribosomes and their subunits obtained by the sandwich technique shows that the *A. salina* ribosomal particles are approximately 15% larger than the corresponding *E. coli* particles.

The prolate ellipsoid shape of the small subunits of both *A. salina* and *E. coli* predetermines their deposition on the supporting film but does not limit their orientation along the horizontal axis. The similarity of the small *A. salina* and *E. coli* subunits in the frontal views is striking. The lateral views, on the other hand, reveal significant structural differences between these subunits. The beak-like protrusion in the upper third and the broad base of *A. salina* subunits are not found in the *E. coli* particles. The beak and the complex structure seem to be common features of other small eukaryotic subunits (unpublished results). However, since no data are available on the properties and topography of individual *A. salina* proteins, no conclusions can be drawn regarding the distribution of the protein and RNA moieties or their involvement in protein synthesis as in the case of *E. coli* subunits (see refs. 1 and 2 for refs.).

Comparison of the three-dimensional structure of large *A. salina* and *E. coli* subunits is limited because of the dominant orientation of 50S *E. coli* subunits in the "crown" view. The smaller right-hand side crest of 60S *A. salina* subunits may enhance their roundness and explain the lack of an obvious preferential orientation. The split in the left-hand side crest of 50S *E. coli* subunits leads to speculation on its possible relation to the site of L7/L12 dimers (14). The unique properties of proteins L7/L12, e.g., the presence of three to four copies per 50S *E. coli* subunit (15, 16), the highly helical structure (17, 18),

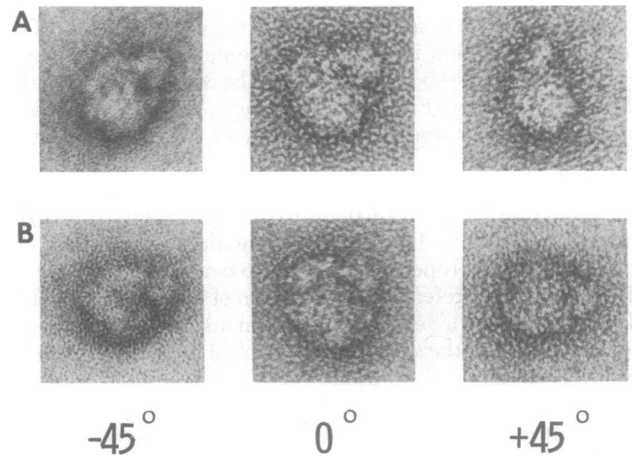

FIG. 7. 80S *A. salina* monosomes in buffer A, stained with 0.5% aqueous uranyl acetate and tilted ± 45° (*A*) along the vertical axis and (*B*) along the horizontal axis. (Both ×495,000.)

and the necessity for factor-dependent GTP hydrolysis (19), make their topography of prime interest. We have established that proteins L7/L12 are located in both side crests of the 50S subunit (11), while others report that these proteins are present only in one side crest (10) or are located in the central protuberance (2). Experiments to determine the location of *A. salina* proteins EL7/EL12, equivalent to *E. coli* proteins L7/L12 (20) are in progress. We have not succeeded in topographically mapping these proteins by immunoelectron microscopy using antibodies against *E. coli* L7/L12. The stoichiometry of EL7/EL12 is yet to be determined; preliminary data suggest the presence of less than one copy per 60S *A. salina* subunit (20).

It is known that the base of the large subunits is the attachment site of the ribosomes to the membrane during protein synthesis. The knob-like protrusion, first found in the base of the 60S *A. salina* subunit, raises the question whether this structure may be involved in the transfer of synthesized protein across the membrane (21, 22). The fact that this protrusion has not been observed on 50S *E. coli* subunits and on 80S *A. salina* monosomes should be clarified by tilting experiments.

Except in size, *A. salina* and *E. coli* monosomes do not strikingly differ in overall appearance. The protuberance resolved in some 60S *A. salina* subunits after assembly in the 80S monosome (Fig. 5*A* 2 and 7) could be the result of interactions with the 40S subunit. The significance of this structural feature is not known. Electron micrographs of *A. salina* monosomes in the "crown" view suggest an association of subunits similar to that observed in *E. coli* monosomes (8): the small subunit is situated in the crown region of the large subunit lengthwise between the two side crests, with the one-third partition directed toward the left-hand side crest. The cavity between the three crests of the large subunit does not show any structure that would imply a preferential site for the accomodation of the small subunit. Our recent electron microscopic studies on the structure of functional prokaryotic–eukaryotic hybrid ribosomes (unpublished observations) support the view that there is an extensive structural similarity between prokaryotic and eukaryotic ribosomes.

Our model for the arrangement of subunits in the monosome differs from that proposed by Lake for 70S *E. coli* ribosomes (10). In Lake's model the small subunit is located with the platform in an indentation of the large subunit, rotated by about 90° as compared to our model. The assembly of the subunits on the monosome is of particular interest since it determines the interface that is the suggested site of protein synthesis (23). The interface in our model also differs from that in the model of Tischendorf *et al.* (2, 24), mainly because we have found asymmetry for both *E. coli* subunits. It should be mentioned that the interface is still a vaguely defined structure. From electron microscopy it is evident that the space between both subunits is sufficient to accomodate tRNAs, mRNA, and "factors" involved in protein synthesis. However, any other conclusions regarding their mutual orientation in this process are highly speculative.

We thank Dr. Severo Ochoa for his helpful discussion and Dr. J. M. Sierra and Miss C. Melcharick for the *A. salina* ribosomes. We also gratefully acknowledge JEOL (USA), Inc. for the use of JEM 100C and Mr. J. O. Yoshioka for his expert cooperation in the tilting experiments.

1. Kurland, C. G. (1977) *Annu. Rev. Biochem.* **46,** 173–200.
2. Stöffler, G. & Wittmann, H. G. (1977) in *Molecular Mechanism of Protein Synthesis* eds. Weissbach, H. & Pestka, S. (Academic, New York) pp. 117–202.
3. Wool, I. G. & Stöffler, G. (1974) in *Ribosomes* eds. Nomura, M., Tissiéres, A. & Lengyel, P. (Cold Spring Harbor Lab. Press, New York) pp. 417–460.
4. Lake, J. A., Sabatini, D. D. & Nonomura, Y. (1974) in "Ribosomes" eds. Nomura, M., Tissiéres, A. & Lengyel, P. (Cold Spring Harbor Lab. Press, New York) p. 547.
5. Zasloff, M. & Ochoa, S. (1971) *Proc. Natl. Acad. Sci. USA* **68,** 3059–3063.
6. Pestka, S. & Nirenberg, M. (1966) *J. Mol. Biol.* **21,** 145–171.
7. Brot, N., Yamasaki, E., Redfield, B. & Weissbach, H. (1970) *Biochem. Biophys. Res. Commun.* **40,** 698–707.
8. Boublik, M., Hellmann, W. & Kleinschmidt, A. K. (1977) *Cytobiologie* **14,** 293–300.
9. Wabl, M. R., Barends, P. J. & Nanninga, N. (1973) *Cytobiologie* **7,** 1–9.
10. Lake, J. (1976) *J. Mol. Biol.* **105,** 131–159.
11. Boublik, M., Hellmann, W. & Roth, H. E. (1976) *J. Mol. Biol.* **107,** 479–490.
12. Tischendorf, G. W., Zeichhardt, M. & Stöffler, G. (1974) *Mol. Gen. Genet.* **134,** 187–208.
13. Nonomura, Y., Blobel, G. & Sabatini, D. (1971) *J. Mol. Biol.* **60,** 303–323.
14. Österberg, R., Sjöberg, B., Liljas, A. & Pettersson, I. (1976) *FEBS Lett.* **66,** 48–51.
15. Thammana, P., Kurland, C. G., Deusser, E., Weber, J., Maschler, R., Stöffler, G. & Wittmann, H. G. (1973) *Nature New Biology* **242,** 47–49.
16. Hardy, J. S. (1975) *Mol. Gen. Genet.* **140,** 253–274.
17. Dzionara, M. (1970) *FEBS Lett.* **8,** 197–200.
18. Boublik, M., Brot, N. & Weissbach, H. (1973) *Biopolymers* **12,** 2083–2092.
19. Möller, V. (1974) in *Ribosomes* eds., Nomura, M., Tissiéres, A. S. & Lengyel, P., (Cold Spring Harbor Lab. Press, New York) pp. 711–731.
20. Möller, W., Slobin, L. I., Amons, R. & Richter, D. (1975) *Proc. Natl. Acad. Sci. USA* **72,** 4744–4748.
21. Sabatini, D. D., Tashiro, Y. & Palade, G. E. (1966) *J. Mol. Biol.* **19,** 503–524.
22. Blobel, G. & Dobberstein, B. (1975) *J. Cell Biol.* **67,** 835–851.
23. Ochoa, S. (1976) *Naturwissenschaften* **63,** 347–355.
24. Tischendorf, G. W., Zeichhardt, H. & Stöffler, G. (1975) *Proc. Natl. Acad. Sci. USA* **72,** 4820–4824.